Advanced Physical Research
Vol.8, No.1, 2026, pp.30-39
https://doi.org/10.62476/apr.8130

Jomard Publishing

A STUDY OF RADIAL ELECTRON DENSITY AND ONE–ELECTRON EXPECTATION VALUES FOR THE $2s^2$ CONFIGURATION IN ATOMS WITH $4 \leq Z \leq 15$

Mayada J. AL-Sharaa[1*], **Khamael Ibrahim Abdulwahid**[1],
Qassim Shamkhi Al Khafaji[2], **Shaymaa Awad Kadhim**[2]

[1]Department of Physics, College of Science, University of Misan, Misan, Iraq
[2]Department of Physics, Faculty of Science, University of Kufa, Najaf, Iraq

Abstract. In this study, the Hartree–Fock–Ruthan method was used with Slater-type orbitals to examine a group of atoms and ions with atomic numbers from $Z = 4$ to $Z = 15$. The main calculations focused on the radial electron density distribution, several expectation values of $\langle r_1^n \rangle$, and the nuclear magnetic shielding constant. The results show clear changes in the shape of the electron density and in the position of its main peaks as the nuclear charge increases. The values $\langle r_1^n \rangle$ of and the shielding constant also changed in a regular way across the studied atoms and ions. These results provide a simple view of how some electronic properties vary when the nuclear charge becomes larger.

Keywords: Nuclear magnetic shielding constant, radial electron density, Hartree–Fock method.
Corresponding author: Mayada J. AL-Sharaa, Department of Physics, College of Science, University of Misan, Misan, Iraq, e-mail: *mayadajassim@uomisan.edu.iq*
Received: 16 December 2025; Revised: 16 January 2026; Accepted: 26 January 2026; Published: 18 February 2026.

1 Introduction

The behavior of electrons inside atoms cannot be explained by classical ideas, because electrons move in ways that follow the rules of quantum mechanics. Schrödinger introduced his well-known wave equation in 1926, and this equation became the basic tool for studying atoms at the microscopic level (Schrödinger & Works, 1926). For atoms that have only one electron, such as the hydrogen atom, the equation can be solved exactly. But when an atom contains more than one electron, the repulsion between electrons makes the problem too complicated for an exact solution, so several approximate methods were developed.

One of the early attempts was made by Hartree, who suggested writing the total wave function as a product of single-electron functions (Blinder, 2019). This helped simplify the problem, but it did not satisfy the anti-symmetry condition required for electrons. Later, Slater and Fock introduced the idea of using a determinant to build a wave function that automatically satisfies anti-symmetry (Morrison & Kobus, 2018). This led to the Hartree–Fock (HF) method, which is now a common approach in atomic structure calculations (Fano & Blinder, 2017). The HF method assumes that each electron moves in an average field created by all the other electrons. Even though this method does not include all correlation effects, it still gives good estimates of many atomic properties (Pisani et al., 2012). In practical calculations, Slater-type orbitals (STOs) are often used because they have the right behavior near the nucleus and decrease smoothly at larger distances (Sharma, 2021; West et al., 2013).

Many earlier studies have used HF and STO functions to examine electron density and correlation in different atoms and ions. For example, (AL-Jabri & AL-Khafaji, 2014), studied correlation energy and electron density at the nucleus for several highly charged ions. In another study, (AL-Bayati et al., 2015), examined electron correlation in inter-shell transitions using the radial function $f(r_1^2)$.

Recent investigations have also employed radial electron density analysis to explore correlation and relativistic effects in atomic systems, as demonstrated in the work of (Schiffmann et al., 2022). In addition, (AL-Sharaa et al., 2025) investigated the atomic properties of ten-electron systems for the neon atom and its isoelectronic ions using Hartree–Fock methods, demonstrating the influence of increasing nuclear charge on radial behavior and related atomic parameters. This study further supports the importance of HF-based approaches in analyzing electron distributions across atomic sequences (AL-Sharaa et al., 2025).

In this work, the Hartree–Fock–Ruthan method is applied to atoms and ions with atomic numbers between $Z = 4$ and $Z = 15$. The study focuses on calculating the radial electron density distribution $D(r_1)$, the expectation values $\langle r_1^n \rangle$ for the $2s^2$ configuration, and the nuclear magnetic shielding constant. All calculations were carried out using Mathcad 2001i in atomic units. The results show clear and regular changes in these properties as the nuclear charge increases.

Recent atomic studies using the Hartree–Fock method have examined radial electron density and related expectation values, confirming the continued use of this approach in atomic structure studies Schiffmann et al. (2022); Santra & Obermeyer (2021).

2 Research Gap

Although several earlier studies have examined electron density, correlation effects, or expectation values for selected atoms and ions, most of these works were limited to specific charge states or to inner-shell electrons such as 1s or 2p. Only a few papers have considered the $2s^2$ configuration across a continuous atomic sequence, and none of them combined the calculation of the radial density $D(r_1)$, the one-electron moments $\langle r_1^n \rangle$, and the nuclear magnetic shielding constant within the same study.

This lack of a combined and systematic treatment forms the main gap that the present work aims to fill.

3 Novelty of the Work

The novelty of this work lies in combining three important atomic properties within one study: the radial electron density, the one-electron expectation values $\langle r_1^n \rangle$, and the nuclear magnetic shielding constant. These quantities were calculated for the $(2s^2)$ configuration across the atomic range $4 \leq Z \leq 15$ using the same Hartree–Fock–Ruthan approach. Earlier studies usually examined only one of these properties or focused on limited charge states, whereas the present work provides a unified and systematic analysis of these properties within a single computational framework. This combination gives a clearer and more complete picture of how these electronic properties vary with the nuclear charge.

4 Theoretical Part

The quantum mechanical description of a multi-electron atom begins with the stationary Schrödinger equation.

$$\psi \hat{H} = E\psi \tag{1}$$

where ψ is the electronic wave function and $\hat{H}$ is the Hamiltonian operator containing kinetic energy terms, electron–nucleus attraction, and electron–electron repulsion. Due to the coupling introduced by the term $\frac{1}{r_{ij}}$ Eq. (1) cannot be solved analytically for systems with more than one electron (Sharma, 2021).

4.1 Hartree approximation

Hartree proposed expressing the wave function as a product of single-electron orbitals (Dias, 2023)

$$\phi_i(i) \prod_{i=1}^{N} \Psi_H(1, 2 \ldots N). \tag{2}$$

This describes each electron as moving in an averaged potential created by all others. However, Eq. (2) fails to satisfy anti-symmetry and, consequently, the Pauli exclusion principle.

4.2 Slater determinant and Hartree–Fock method

Slater and Fock corrected the symmetry deficiency by proposing an anti-symmetric wave function written as a Slater determinant (Fischer et al., 2007).

$$\psi(1, 2, 3, \ldots, N) = \frac{1}{\sqrt{N!}} \begin{vmatrix} \phi_1(1) & \phi_1(2) & \ldots & \phi_1(N) \\ \phi_2(1) & \phi_2(2) & \ldots & \phi_2(N) \\ \vdots & \vdots & \vdots & \vdots \\ \phi_N(1) & \phi_N(2) & \ldots & \phi_N(N) \end{vmatrix} \tag{3}$$

The Slater determinant is used to ensure that the total wave function remains antisymmetric under the exchange of two electrons, a fundamental requirement imposed by the Pauli exclusion principle. This determinant provides the standard representation of the multi-electron wave function by constructing it from a set of single-electron orbitals, each associated with an electron and its spin, thereby offering an appropriate description of the quantum state of the system.

The theoretical formulation of the Hartree–Fock method, as well as the incorporation of the Slater determinant within it, follows the standard presentation given by (Szabo & Ostlund, 1996), which is considered one of the foundational references in electronic structure theory. Substituting the Slater determinant into the electronic Schrödinger equation leads to a set of coupled integro-differential equations that must be solved to obtain the single-electron orbitals. Each spin-orbital is then defined according to the following expression:

$$\chi_i = \phi_i(r)\, w_i(s) \tag{4}$$

Minimization of the expectation value of the Hamiltonian yields the Hartree–Fock equations, solved iteratively until self-consistency is achieved (Cowan, 2023).

4.3 Slater-type orbitals (STOs)

A normalized STO is expressed as (Johnson, 2007).

$$\chi_{nlm}(r, \theta, \phi) = N_n r^{n-1} e^{\zeta r -} Y_{lm}(\theta, \phi) \tag{5}$$

where n is the principal quantum number, ζ is the orbital exponent, and Y_{lm} are spherical harmonics. HF orbitals are expanded using multiple STOs (Lietz et al., 2017).

$$\phi_i = \sum_j C_i \chi_{ij} \tag{6}$$

4.4 Radial electron density distribution

The radial density distribution is given by (Lehtola, 2019).

$$D\left(r_1\right) = r_1^2 \int \left|\psi\left(r_1, \Omega_1\right)\right|^2 d\Omega_1 \tag{7}$$

$$\rho\left(r_1\right) = \int \left|\psi\left(r_1, \Omega_1\right)\right|^2 d\Omega_1 \tag{8}$$

The function $\rho(r_1)$ represents the one–electron density at a radial distance r_1. It is obtained by integrating the total normalized wave function over all angular coordinates, which removes the angular dependence and leaves only the radial contribution to the probability density. This definition expresses the probability of finding an electron within an infinitesimal spherical shell at radius r_1, independent of its angular position (Bransden & Joachain, 2003).

Accordingly, the radial electron density distribution $D(r_1)$ is written as:

$$D\left(r_1\right) = \rho\left(r\right) r_1^2 \tag{9}$$

which incorporates the Jacobean factor r_1^2 arising from the transformation to spherical coordinates. The function $D(r_1)$ describes the probability of locating an electron between radii r_1 and $r_1 + dr_1$, and the positions of its maxima provide valuable information about the most probable electron–nucleus distances (Al-Sharaa et al., 2017).

4.5 One-particle expectation value $\langle r_1^n \rangle$

One may compute the one-particle expectation value $\langle r_1^n \rangle$ from (AL-Quraishi & AL-Khafaji, 2022).

$$\langle r_1^n \rangle = \int D_{ij}\left(r_1\right) r_1^n dr_1 \tag{10}$$

When $(n = 0)$ is the case, the Normalization condition can be calculated because $\langle r_1^n \rangle$ is one .

4.6 Nuclear magnetic shielding constant

The average shielding that a specific atom (or an atom in a molecule) will experience in a magnetic field can be calculated with the help the constant of nuclear magnetic shielding (Heine et al., 2005), In nuclear magnetic resonance (NMR) spectroscopy, where the chemical spectra are used as a "fingerprint" technique, this information is crucial.In chemistry, NMR is arguably the most significant instrument (Jaszuński et al., 2012; Ramsey, 1950).

σ_d is determined from the formula

$$\sigma_d = \frac{\alpha^2}{3} \left\langle \psi \left| \sum_{i=1}^{n} \left(r_i\right)^{-1} \right| \psi \right\rangle \tag{11}$$

Where α is the fine –structure constant ,whose value is taken as $(7.297353 * 10^{-3})$ (Engström et al., 1998).

5 Computational Details

The calculations were carried out for the valence (2s) orbital, which contains two electrons forming a closed-shell ($2s^2$) configuration. Slater-type orbitals were used to represent the radial wavefunction, and the orbital parameters were taken from published Hartree–Fock atomic tables reported in the literature and kept fixed during the calculations (Macchi & Coppens, 2001). All wavefunctions were properly normalized, and the required expectation values were evaluated using standard Hartree–Fock procedures implemented in Mathcad.

6 Results and Discussions

In this study, the radial electron density distribution $D(r_1)$, the one-particle expectation values for the ($2S^2$) configuration, and the nuclear magnetic shielding constant were calculated for a set of atoms and ions with atomic numbers from $Z = 4$ to $Z = 15$. All calculations were carried out using the Hartree–Fock wave functions implemented in Mathcad 2001.

Table 1: Values of positions and maximum values of $D(r_1)$ by using Hartree -Fock wave function

Atom	z	r_1	$D(r_1)_{max}$	Atom	z	r_1	$D(r_1)_{max}$
Be	4	0.22 2.05	0.0599 0.3957	F	9	0.092 0.764	0.1978 1.0551
B^{+1}	5	0.16 1.43	0.0992 0.6019	Ne^{+1}	10	0.087 0.674	0.2395 1.2393
C^{+2}	6	0.14 1.12	0.1476 0.8016	Na^{+2}	11	0.074 0.598	0.2869 1.4272
B	5	0.202 1.52	0.0785 0.5329	Ne	10	0.087 0.685	0.2253 1.1847
C^{+1}	6	0.15 1.18	0.1264 0.7294	Na^{+1}	11	0.077 0.619	0.2689 1.3647
N^{+2}	7	0.12 0.99	0.1752 0.9219	Mg^{+2}	12	0.071 0.553	0.3139 1.5525
C	6	0.143 1.194	0.1209 0.6765	Na	11	0.083 0.616	0.2643 1.3660
N^{+1}	7	0.121 0.99	0.1551 0.8555	Mg^{+1}	12	0.073 0.556	0.3122 1.552
O^{+2}	8	0.102 0.83	0.2026 1.0493	Al^{+2}	13	0.064 0.505	0.3615 1.7398
N	7	0.121 1.035	0.1387 0.7913	Mg	12	0.077 0.557	0.307 1.5523
O^{+1}	8	0.101 0.86	0.183 0.9811	Al^{+1}	13	0.067 0.501	0.359 1.7414
F^{+2}	9	0.09 0.742	0.2301 1.1737	Si^{+2}	14	0.061 0.456	0.456 1.9315
O	8	0.109 0.863	0.168 0.9243	Al	13	0.066 0.504	0.3597 1.7398
F^{+1}	9	0.099 0.755	0.209 1.1109	Si^{+1}	14	0.063 0.46	0.4039 1.9281
Ne^{+2}	10	0.089 0.667	0.255 1.3001	P^{+2}	15	0.055 0.424	0.4568 2.1164

Table 1 lists the positions of the maxima of $D(r_1)$ together with their corresponding values. The general trend shows that the maximum value of the radial density increases when the atomic number becomes larger. At the same time, the position of this maximum shifts closer to the nucleus. This behavior agrees with the Coulombic attraction, since a larger nuclear charge pulls the electron cloud closer and makes the density more compact.

Figure 1 shown how $D(r_1)$ varies with position for all atoms and ions studied. Two peaks can be observed in each curve. The small peak at short distances is related to the penetration of the 2s electron toward the nucleus, which makes it spend a short time in a region usually associated with the 1s orbital. The second and larger peak corresponds to the main location of the 2s electron. In all curves, $D(r_1)$ becomes zero at $r_1 = 0$, meaning that the electron cannot exist at the nucleus. The function also approaches zero when r_1 becomes very large, which is consistent with the fact that the electron remains inside the atom.

Table 2: The one- particle expectation values $\langle r_1^n \rangle$ for atoms $-2 \geq n \geq 2$.

Atom	z	$\langle r_1^{-2} \rangle$	$\langle r_1^{-1} \rangle$	$\langle r_1^{0} \rangle$	$\langle r_1^{1} \rangle$	$\langle r_1^{2} \rangle$
Be	4	1.155452	0.531828	1.000077	2.647430	8.423246
B^{+1}	5	2.415014	0.780148	1.000001	1.798191	3.825901
C^{+2}	6	4.283678	1.034139	1.000009	1.371967	2.214758
B	5	2.024482	0.712883	1.000000	1.977064	4.709127
C^{+1}	6	3.717948	0.961175	1.000009	1.475565	2.589839
N^{+2}	7	5.930802	1.211368	0.999997	1.178844	1.642740
C	6	3.501118	0.920849	1.000000	1.560654	2.937004
N^{+1}	7	5.288757	1.140839	0.999997	1.252841	1.874552
O^{+2}	8	7.847578	1.388554	0.999986	1.033710	1.267941
N	7	4.754181	1.078189	1.000011	1.332295	2.149463
O^{+1}	8	7.127716	1.319794	0.999993	1.089277	1.421228
F^{+2}	9	10.029845	1.565729	1.000001	0.920615	1.008797
O	8	6.592131	1.265261	1.000005	1.142031	1.581591
F^{+1}	9	9.295806	1.503315	0.999995	0.960880	1.108377
Ne^{+2}	10	12.539865	1.746762	0.999996	0.828155	0.818212
F	9	8.6985860	1.4497271	0.9999	1.0010153	1.2162369
Ne^{+1}	10	11.735175	1.685534	1.000003	0.860330	0.890547
Na^{+2}	11	15.317820	1.927169	1.000012	0.752954	0.677976
Ne	10	11.071131	1.632546	1.000010	0.892132	0.967168
Na^{+1}	11	14.452271	1.866985	0.999999	0.779077	0.731234
Mg^{+2}	12	18.370181	2.107153	0.999995	0.690353	0.570886
Na	11	14.451368	1.867191	0.999994	0.779111	0.731631
Mg^{+1}	12	18.371954	2.107090	1.000001	0.690599	0.571621
Al^{+2}	13	22.810069	2.349694	0.999998	0.619831	0.458607
Mg	12	18.383246	2.107758	1.000002	0.690360	0.571166
Al^{+1}	13	22.828965	2.350636	1.000001	0.619552	0.458109
Si^{+2}	14	27.782933	2.595190	1.000007	0.561814	0.375533
Al	13	22.784738	2.348575	1.000003	0.620016	0.458874
Si^{+1}	14	27.717107	2.591943	0.999987	0.562527	0.376656
P^{+2}	15	33.150186	2.836365	1.000006	0.514713	0.314596

Table 2 shows the one-particle expectation values $\langle r_1^{-1} \rangle$ for different values of n. The results indicate that when n is negative (-1 or -2), the expectation values increase with increasing atomic number. When n is positive (+1 or +2), the values also rise with Z, but the size of the change varies depending on whether the exponent emphasizes regions close to or far from the nucleus. These behaviors reflect how the electron cloud contracts as the nuclear charge increases.

Table 3: Nuclear magnetic shielding constant

Atom	z	$\sigma_d * 10^{-6}$	Atom	z	$\sigma_d * 10^{-6}$
Be	4	9.430300	F	9	25.706358
B^{+1}	5	13.833475	Ne^{+1}	10	29.887653
C^{+2}	6	18.337208	Na^{+2}	11	34.172291
B	5	12.640742	Ne	10	28.948077
C^{+1}	6	17.043420	Na^{+1}	11	33.105117
N^{+2}	7	21.479808	Mg^{+2}	12	37.363742
C	6	16.328366	Na	11	33.108769
N^{+1}	7	20.229197	Mg^{+1}	12	37.362625
O^{+2}	8	24.621645	Al^{+2}	13	41.664445
N	7	19.118296	Mg	12	37.374470
O^{+1}	8	23.402402	Al^{+1}	13	41.681148
F^{+2}	9	27.763287	Si^{+2}	14	46.017546
O	8	22.435431	Al	13	41.644603
F^{+1}	9	26.656571	Si^{+1}	14	45.959970
Ne^{+2}	10	30.973339	P^{+2}	15	50.294027

The nuclear magnetic shielding constant values are presented in Table 3. A clear increase

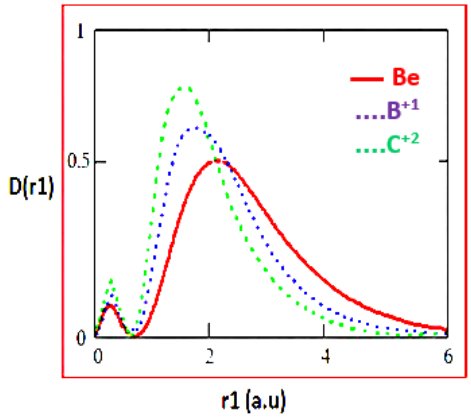
D(r1)
r1 (a.u)
Be
B+1
C+2

(a)

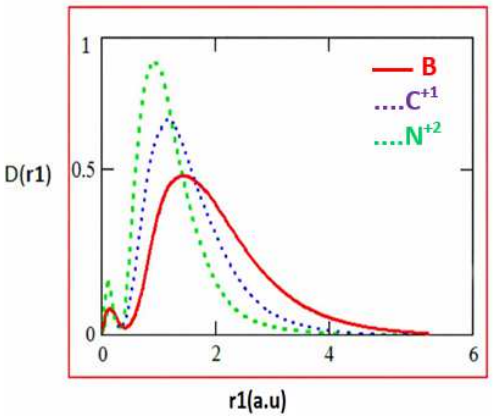
D(r1)
r1(a.u)
B
C+1
N+2

(b)

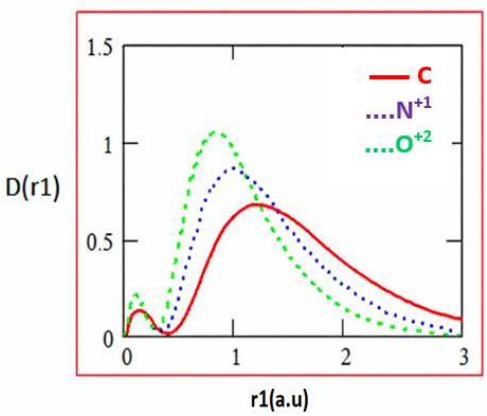
D(r1)
r1(a.u)
C
N+1
O+2

(c)

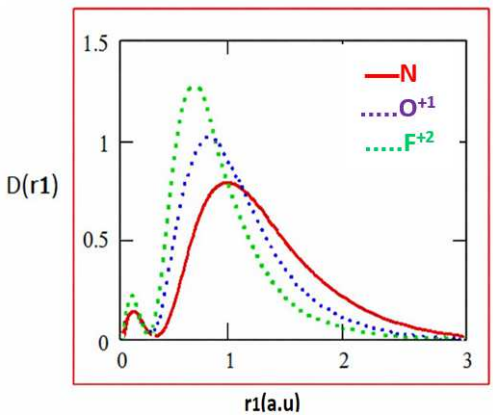
D(r1)
r1(a.u)
N
O+1
F+2

(d)

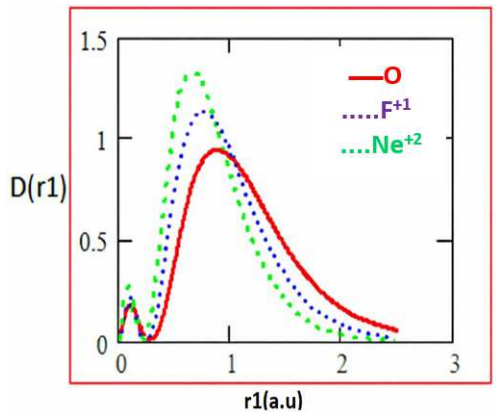
D(r1)
r1(a.u)
O
F+1
Ne+2

(e)

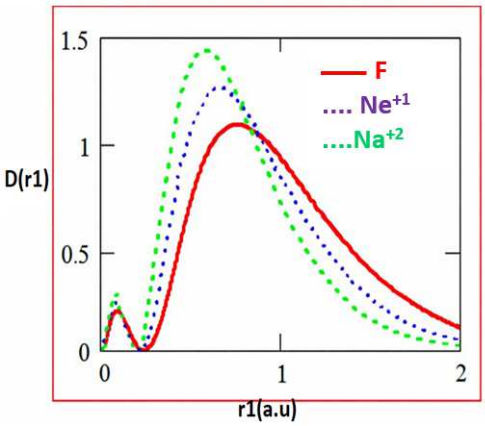
D(r1)
r1(a.u)
F
Ne+1
Na+2

(f)

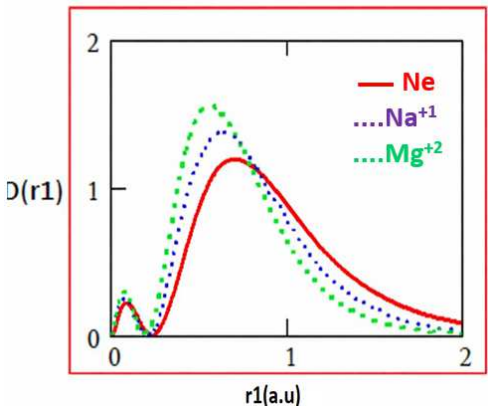
D(r1)
r1(a.u)
Ne
Na+1
Mg+2

(g)

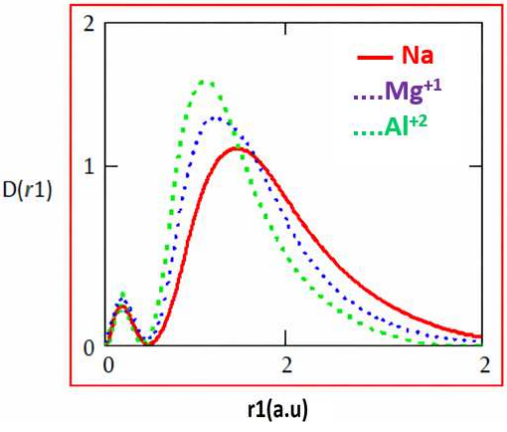
D(r1)
r1(a.u)
Na
Mg+1
Al+2

(h)

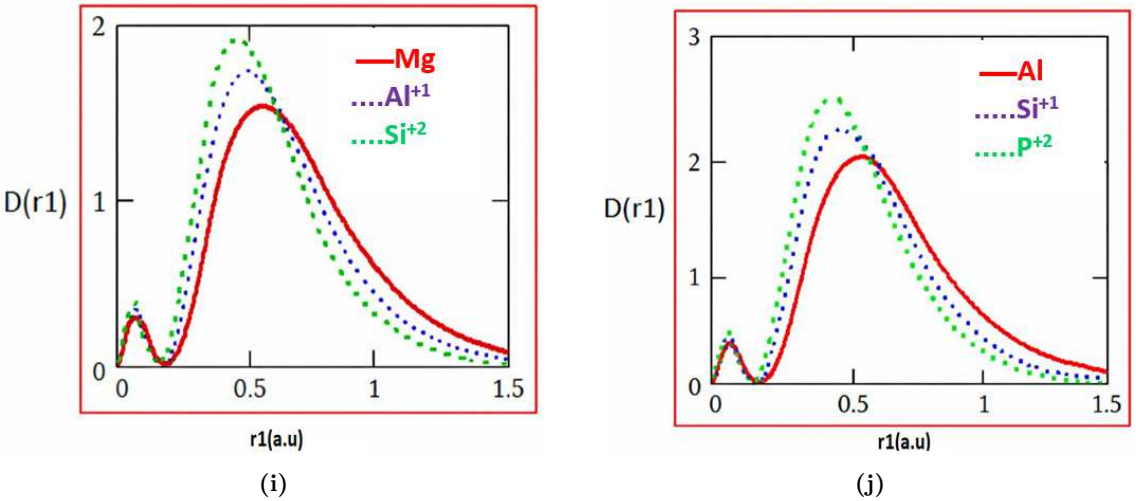

Figure 1: One-electron radial density distribution $D(r_1)$ as a function of radial distance r_1: (a) for Be and like ion, (b) for B and like ion, (c) C and like ion, (d) N and like ion, (e) O and like ion, (f) F and like ion, (g) Ne and like ion, (h) Na and like ion, (i) Mg and like ion, (j) Al and like ion. The radial distance r_1 is given in atomic units (a.u.).

is observed as Z increases. This is expected because a higher nuclear charge creates a stronger attraction between the nucleus and the electron, which reduces the effective magnetic field at the nucleus and results in a larger shielding constant. The close agreement between different charge states of the same element also reflects the reliability of the Hartree–Fock calculations used in this work.

Overall, the results show consistent and systematic trends across the entire atomic sequence. The radial density becomes more concentrated, the expectation values behave regularly with Z, and the magnetic shielding constant increases steadily as the atomic number grows. These observations match well with previous theoretical studies and support the applicability of the Hartree–Fock–Ruthan approach for this type of atomic analysis.

7 Conclusion

In this work, the Hartree–Fock–Ruthan method with Slater-type orbitals was used to study a number of atoms and ions in the range $Z = 4$ to $Z = 15$. The main quantities examined were the radial electron density distribution, the expectation values $\langle r_1^1 \rangle$ for the $2s^2$ configuration, and the nuclear magnetic shielding constant.

The results showed that the radial density becomes more compact as the nuclear charge increases, with the position of the density maximum moving closer to the nucleus. The expectation values followed regular and understandable trends for both positive and negative powers of r_1, which reflects how the electron cloud changes in size as Z increases. In addition, the nuclear magnetic shielding constant increased steadily across the studied atoms and ions, in line with the known effect of stronger nuclear attraction on the local magnetic field.

Overall, the findings give a clear and simple picture of how several atomic properties depend on the nuclear charge. The agreement of the trends with previous studies indicates that the Hartree–Fock–Ruthan approach provides reliable results for this type of atomic system.

8 Acknowledgement

The authors would like to express their sincere thanks to the University of Misan, Faculty of Science, for providing partial support and the necessary facilities to complete this work.

9 Ethical Approval

This study does not involve human subjects or animal experiments. Ethical approval was granted by the local institutional committee.

References

AL-Bayati, K.H., Kareem, A.A. & Madhkoor, N.C.H. (2015). Calculation of radial electron–electron distribution function and expectation values for Li-atom in excited states 1s 2p, 1s 3p and 1s 3d. *Baghdad Science Journal*, *12*(3), 19.

AL-Jabri, H.A., AL-Khafaji, Q. (2014). Evaluation of the electron density at the nucleus and the correlation energy in position space. *Journal of Applied Physics*, *6*(2), 59–66.

AL-Quraishi, M.H., AL-Khafaji, Q.S. (2022). Evaluation of the Hartree–Fock energy of four electron systems. *NeuroQuantology*, *20*(6), 4115–4121.

AL-Sharaa, I.D.M.J., Shamkhi, A.F. & AL-Quraishi, M.H. (2025). Estimation of atomic properties of ten-electron systems for neon atom and like ions. *Advanced Physical Research*, *7*(1), 35–47.

Al-Sharaa, M.J., Mahmood, M.A., Madhkoor, N.C. & Al-Bayati, K.H. (2017). Energy calculation for beryllium atom in different excited states ($1s^2$ 2s 3s), (1s $2s^2$ 3s), and (1s 2s $3s^2$). *AIP Conference Proceedings*, *1888*(1), 020013.

Blinder, S.M. (2019). Chapter 1 - Introduction to the Hartree-Fock method. In S.M. Blinder & J.E. House (Eds.), *Mathematical Physics in Theoretical Chemistry* (pp. 1–30). Elsevier.

Bransden, B.H., Joachain, C.J. (2003). *Physics of Atoms and Molecules*. Harlow, UK: Prentice Hall.

Cowan, R.D. (2023). *The Theory of Atomic Structure and Spectra* (Vol. 3). Berkeley, CA, USA: University of California Press.

Dias, E.O. (2023). Space-time-symmetric quantum mechanics in 3+1 dimensions. *arXiv preprint arXiv:2308.04376*.

Engström, M., Minaev, B., Vahtras, O. & Ågren, H. (1998). Linear response calculations of electronic g-factors and spin-rotational coupling constants for diatomic molecules with a triplet ground state. *Chemical Physics*, *237*(1–2), 149–158.

Fano, G., Blinder, S. (2017). *Twenty-First Century Quantum Mechanics: Hilbert Space to Quantum Computers: Mathematical Methods and Conceptual Foundations*. Berlin, Heidelberg, Germany: Springer.

Fischer, C.F., Tachiev, G., Gaigalas, G. & Godefroid, M.R. (2007). An MCHF atomic-structure package for large-scale calculations. *Computer Physics Communications*, *176*(8), 559–579.

Heine, T., Corminboeuf, C. & Seifert, G. (2005). The magnetic shielding function of molecules and Pi-electron delocalization. *Chemical Reviews*, *105*(10), 3889–3910.

Jaszuński, M., Antušek, A., Garbacz, P., Jackowski, K., Makulski, W. & Wilczek, M. (2012). The determination of accurate nuclear magnetic dipole moments and direct measurement of NMR shielding constants. *Progress in Nuclear Magnetic Resonance Spectroscopy*, *67*, 49–63.

Johnson, W. (2007). *Atomic Structure Theory: Lectures on Atomic Physics*. Berlin/Heidelberg, Germany: Springer.

Lehtola, S. (2019). Fully numerical Hartree–Fock and density functional calculations. II. Diatomic molecules. *International Journal of Quantum Chemistry*, *119*(19), e25944.

Lietz, J.G., Novario, S., Jansen, G.R., Hagen, G. & Hjorth-Jensen, M. (2017). Computational nuclear physics and post Hartree-Fock methods. In M. Hjorth-Jensen, M. Lombardo & U. van Kolck (Eds.), *An Advanced Course in Computational Nuclear Physics* (Lecture Notes in Physics, vol. 936). Cham: Springer.

Morrison, J.C., Kobus, J. (2018). Numerical Hartree–Fock and many-body calculations for diatomic molecules. In *Advances in Quantum Chemistry* (Vol. 76, pp. 103–116). Academic Press.

Macchi, P., Coppens, P. (2001). Relativistic analytical wave functions and scattering factors for neutral atoms beyond Kr and for all chemically important ions up to I^-. *Foundations of Crystallography*, *57*(6), 656–662.

Pisani, C., Dovesi, R. & Roetti, C. (2012). *Hartree–Fock Ab Initio Treatment of Crystalline Systems*. Springer.

Ramsey, N.F. (1950). Magnetic shielding of nuclei in molecules. *Physical Review*, *78*(6), 699.

Santra, R., Obermeyer, M. (2021). A first encounter with the Hartree–Fock self-consistent-field method. *American Journal of Physics*, *89*(4), 426–436.

Schiffmann, S., Li, J., Ekman, J., Gaigalas, G., Godefroid, M., Jönsson, P. & Bieroń, J. (2022). Relativistic radial electron density functions and natural orbitals from GRASP2018. *Computer Physics Communications*, *278*, 108403.

Schrödinger, E. & Works, C. (1926). SCHRÖDINGER 1926C. *Annalen der Physik*, *79*, 734.

Sharma, A. (2021). *A Textbook on Modern Quantum Mechanics*. CRC Press.

Szabo, A., Ostlund, N.S. (1996). *Modern Quantum Chemistry*. In *Introduction to Advanced Electronic Structure Theory*. Mineola, NY, USA: Dover Publications, Inc.

West, A.C., Schmidt, M.W., Gordon, M.S. & Ruedenberg, K. (2013). A comprehensive analysis of molecule-intrinsic quasi-atomic, bonding, and correlating orbitals. I. Hartree-Fock wave functions. *The Journal of Chemical Physics*, *139*(23), 234107.